International Journal of Nanomedicine

Dovepress
open access to scientific and medical research

Open Access Full Text Article

ORIGINAL RESEARCH

Iron nanoparticles increase 7-ketocholesterol-induced cell death, inflammation, and oxidation on murine cardiac HL1-NB cells

This article was published in the following Dove Press journal:
International Journal of Nanomedicine
12 March 2010
Number of times this article has been viewed

Edmond Kahn[1]
Mauhamad Baarine[2]
Sophie Pelloux[3]
Jean-Marc Riedinger[4]
Frédérique Frouin[1]
Yves Tourneur[3]
Gérard Lizard[2]

[1]INSERM U678/UMR – S UPMC, IFR 14, CHU Pitié-Salpêtrière, 75634 Paris Cedex 13, France; [2]Centre de Recherche INSERM U866, Equipe Biochimie Métabolique et Nutritionnelle – Université de Bourgogne, Faculté des Sciences Gabriel, 6 Bd Gabriel, 21000 Dijon, France; [3]Centre Commun de Quantimétrie, Université Lyon 1; Université de Lyon, Lyon, France; [4]Département de Biologie et de Pathologie des Tumeurs, Centre Georges François-Leclerc, 21000 Dijon, France

Objective: To evaluate the cytotoxicity of iron nanoparticles on cardiac cells and to determine whether they can modulate the biological activity of 7-ketocholesterol (7KC) involved in the development of cardiovascular diseases. Nanoparticles of iron labeled with Texas Red are introduced in cultures of nonbeating mouse cardiac cells (HL1-NB) with or without 7-ketocholesterol 7KC, and their ability to induce cell death, pro-inflammatory and oxidative effects are analyzed simultaneously.

Study design: Flow cytometry (FCM), confocal laser scanning microscopy (CLSM), and subsequent factor analysis image processing (FAMIS) are used to characterize the action of iron nanoparticles and to define their cytotoxicity which is evaluated by enhanced permeability to SYTOX Green, and release of lactate deshydrogenase (LDH). Pro-inflammatory effects are estimated by ELISA in order to quantify IL-8 and MCP-1 secretions. Pro-oxidative effects are measured with hydroethydine (HE).

Results: Iron Texas Red nanoparticles accumulate at the cytoplasmic membrane level. They induce a slight LDH release, and have no inflammatory or oxidative effects. However, they enhance the cytotoxic, pro-inflammatory and oxidative effects of 7KC. The accumulation dynamics of SYTOX Green in cells is measured by CLSM to characterize the toxicity of nanoparticles. The emission spectra of SYTOX Green and nanoparticles are differentiated, and corresponding factor images specify the possible capture and cellular localization of nanoparticles in cells.

Conclusion: The designed protocol makes it possible to show how Iron Texas Red nanoparticles are captured by cardiomyocytes. Interestingly, whereas these fluorescent iron nanoparticles have no cytotoxic, pro-inflammatory or oxidative activities, they enhance the side effects of 7KC.

Keywords: FAMIS, confocal microscopy, iron nanoparticles, 7-ketocholesterol, SYTOX Green, cardiomyocytes

Introduction

Currently, nanomaterials such as nanotubes, nanowires, fullerene derivatives and quantum dots have received enormous attention to create new types of analytical tools for biotechnology and life sciences.[1–3] Thus, nanomaterials have been used to create unique devices, possessing novel physical and chemical functional properties.[4] Although there are potentially numerous applications of nanomaterials in modern technologies applied to biology and medicine (imaging, delivery of contrast agents, drugs, genes/oligonucleotides and protein/peptides, allowing the monitoring of biodistribution and therapeutic activity, simultaneously),[5,6] there is a serious lack of information concerning their effects on human health especially in patients with cardiovascular risks characterized by elevated plasmatic levels of oxysterols such as 7-ketocholesterol.[7] The main

Correspondence: Edmond Kahn
INSERM U678/UMR-S UPMC,
CHU Pitié-Salpêtrière,
75634 Paris Cedex 13, France
Email kahn@imed.jussieu.fr
or
Gérard Lizard
INSERM 866, Dijon, France
Email gerard.lizard@u-bourgogne.fr

toxicological concern is the fact that some nanoparticles such as iron nanoparticles, are redox active,[4,8,9] and consequently can have some cytotoxic effects on various cellular models,[10,11] and can induce important side effects on small animals.[12,13] Moreover, as some animal models have shown that nanoparticles can access the vascular domain as well as major organs such as brain, kidneys, and liver,[14–16] we asked whether nanoparticles can interact with cardiac cells and induce some cytotoxic effects (induction of cell death, inflammation, and oxidation) on cardiomyocytes to favor cardiac dysfunctions. We also asked whether nanoparticles increase the cytotoxic, pro-inflammatory, and pro-oxidative effects of 7-ketocholesterol (7KC) known to trigger a wide number of side effects on numerous cell types.[17]

Indeed, oxysterols are biologically active molecules resulting from the oxidation of cholesterol. As they penetrate cell membranes, their concentrations can reach harmful levels in various cell types.[7,17] New findings suggest that the effects of oxysterols on cardiomyocytes can lead to cell hypertrophy and death. The pathological actions of oxysterols on smooth muscle cells and cardiomyocytes were shown to depend on dysfunctional Ca^{2+} signalling.[7,17,18] This makes oxysterols one of the major factors precipitating morbidity in cardiac diseases and inflammation-induced heart complications.

Since little information is available on nanomaterial toxicity, simple *in vitro* toxicity models are of major importance especially for iron nanoparticles, which are frequently used to perform medical imaging.[19]

So, the aim of the present *in vitro* study performed on non-beating murine cardiac cells (HL1-NB cells)[20,21] which have been cultured in the absence or in the presence of fluorescent iron nanoparticles labeled with Texas Red associated or not with 7KC, was: 1) to obtain cytological and biochemical information (toxicity, cellular localization) on the effect of these nanoparticles on cardiac cells, and 2) to determine whether they can modulate the biological activity of 7KC itself which is known to contribute to the development of cardiovascular diseases. The cellular interactions able to induce cell death, and the pro-oxidative and pro-inflammatory effects of fluorescent iron nanoparticles associated or not with 7KC after different times of treatment were determined by biochemical techniques, flow cytometry (FCM), and/or confocal laser scanning microscopy (CLSM) coupled with factor analysis of medical image sequences (FAMIS). FAMIS provides factor images corresponding to each fluorescent compound.[22–24] This method uses physical properties of fluorochromes,[25] and enables to isolate and visualize fluorochromes by means of their spectral pattern,[26] as well as their velocity.[27] In the present study, the toxicity was measured with SYTOX Green (0.5 μM; 5-min incubation), which stains dead cells,[28] and by the quantification of lactate dehydrogenase (LDH) activity in the culture medium.[29] Pro-inflammatory effects were evaluated by ELISA via the secretion levels of IL-8 and MCP-1 in the culture medium.[30] Pro-oxidative effects were quantified by flow cytometry with hydroethidine (HE).[31] The kinetics of capture of nanoparticles and SYTOX Green were memorized simultaneously using CLSM during a 10-min period of time. Sequences of images were processed according to a FAMIS based method providing dynamic or spectral components. Sequences of images were obtained according to a protocol requiring either the memorization of an image every 3 or 10 s inside a spectral window, or the scanning along the emission spectrum (525–715 nm). Using these image sequences, the aim of the work was to 1) characterize the incorporation and exit dynamics of nanoparticles, 2) differentiate the emission spectra of SYTOX Green and of nanoparticles. Computed dynamic and spectral curves (factors) and corresponding factor images generated by FAMIS are used to visualize the capture and final localization of nanoparticles in HL1-NB cells.

Our data support that the iron nanoparticles have very slight cytotoxic effects on HL1-NB cells (no increase of SYTOX Green associated fluorescence, slight increase of LDH release), that they are captured by cells, and that they do not stimulate IL-8 and MCP-1 secretion nor reactive oxygen species (ROS) production. However, when associated with 7KC, iron nanoparticles enhance the cytotoxicity as well as the pro-inflammatory and pro-oxidative effects of this compound. Our approach, which can provide a valuable tool to differentiate the biological activities of various nanoparticles associated or not with other compounds in living cells, underlines that iron nanoparticles can reinforce the side effects of potential cardiovascular risk factors such as 7KC.

Materials and methods

Cells, cell culture, and cell treatments

The HL-1 cell line derives from tumoral atrial cardiac myocytes from transgenic mice, and was a gift from Dr WC Claycomb (Louisiana State University Medical Center).[20] HL1-NB cells obtained as described before[21] were cultured in Claycomb medium (JRH Biosciences Ltd.) supplemented with 10% fetal bovine serum, 4 mM L-glutamine, 100 U/mL penicillin, 100 mg/mL streptomycin, 0.3 mM ascorbic acid and 10 mM norepinephrine, at 37 °C in a humid atmosphere of 5% CO_2/95% air. F25 flasks (for cell production), 12 mm glass cover plates (in 35 mm boxes, for microscopy), and 6 wells cell culture plates (for flow cytometry) were coated with

a mixture of gelatin (0.02%) and fibronectin (12.5 mg/L). The Claycomb medium was renewed daily. Cells were split at a mean density of 15,000/cm^2 and were allowed to reach confluence before treatments with iron nanoparticles and/or 7-ketocholesterol (7KC).

7KC was provided by Sigma (L'Isle d'Abeau Chesnes, France). Stock solution of 7KC was prepared at 800 µg/mL: 800 µg of 7KC were dissolved in 50 µL of absolute ethanol, 950 µl of culture medium were added, and the solution was sonicated. To obtain a 40 µg/mL final 7KC concentration (100 µM), 50 µL of the initial solution was added per ml of culture medium on confluent cells. In our culture conditions, confluence was reached at 48 h of culture, and To corresponds to the introduction of 7KC associated or not with MACS iron nanoparticles (Miltenyi Biotec, Germany) in the culture medium.

Iron nanoparticles used at 10 µg/mL final concentration were prepared as follows. MACS nanoparticles (diameters: 20–50 nm), which are goat anti-rabbit IgG microbeads (Miltenyi Biotec, Ref: 130-048-602) were incubated for 30 min at 21 °C with Texas Red conjugated rabbit IgG (Rockland, PA, USA; Ref: 011-0902) in order to obtain fluorescent nanoparticles. Fluorescent nanoparticles were collected with a magnet (STEMCELL Technologies, Grenoble, France), resuspended in distilled water (concentration adjusted at 1 mg/mL), and stored at 4 °C for a period of time not exceeding 6 months. While some iron nanoparticles with a size comprised between 250–300 nm were observed by fluorescence microscopy, the presence of smaller nanoparticles (20–250 nm) is also theoretically highly probable.

Evaluation of cell death by quantification of LDH and by nuclear staining with SYTOX green

HL1-NB confluent cells were cultured with or without fluorescent iron nanoparticles associated or not with 7KC (40 µg/mL) for 30 h, and the release of LDH in the culture supernatants, which increases with cell death, was measured by using a Vitros 950 (Ortho Clinical Diagnostics, Rochester, NY, USA). Moreover, the percentages of SYTOX Green positive cells (corresponding to dead cells) were also simultaneously determined.[32] SYTOX Green (Molecular Probes/Invitrogen, Cergy Pontoise, France) was used at a final concentration of 0.5 µM. After 10 min of incubation at room temperature, the samples were analyzed, and the fluorescence of the dye was collected with a 520/10 nm band pass filter. Data were collected on a logarithmic scale on a GALAXY/PAS flow cytometer (Partec Gmbh, Münster, Germany), and further analyzed with FlowMax software (Partec).

Measurement of IL-8 and MCP-1 secretion by ELISA

To measure interleukin-8 (IL-8) and monocyte chemotactic protein-1 (MCP-1) secretion by ELISA, confluent HL1-NB cells were incubated for 30 h with or without fluorescent iron nanoparticles associated or not with 7KC (40 µg/mL). At the end of the incubation time, the culture medium was collected by centrifugation, and stored at −80 °C. Samples were defrosted just before ELISA was performed in accordance with the procedures of the manufacturers (IL-8: Bender MedSystems™; Vienna, Austria; MCP-1: PeproTech EC, London, UK).

Flow cytometric measurement of the production of reactive oxygen species

The production of reactive oxygen species (ROS) was determined on HL1-NB confluent cells cultured for 30 h with or without iron nanoparticles in the absence or presence of 7KC (40 µg/mL). At the end of the treatment, cells were detached by trypsinization and resuspended in the culture medium at 10^6 cells/mL. To measure the production of ROS, cells were incubated with HE, which allows the identification of superoxide anions. Indeed, HE is a nonfluorescent compound which can diffuse through cell membranes, and which is rapidly oxidized in ethidium under the action of superoxide anions.[33,34] HE (Molecular Probes/Invitrogen, Cergy Pontoise, Paris) was initially prepared at a concentration of 10 mM in DMSO, and was used at a 4 µM final concentration on cell samples of 10^6 cells per ml of culture medium. After 15 min of incubation at 37 °C, 10,000 cells were analyzed by flow cytometry with a GALAXY/PAS flow cytometer (Partec) at excitation and emission wavelengths of 488 nm and 590/10 nm, respectively. Data were collected on a logarithmic scale, and further analyzed with FlowMax software (Partec).

Observation by conventional fluorescence microscopy and fluorescence analysis by confocal laser scanning microscopy

The emission of untreated or of 7KC-treated-HL1-NB cell cultures incubated or injected with MACS Texas Red and stained with SYTOX Green was analyzed by means

of confocal laser scanning microscopy (CLSM) in three-dimensional (3D) sequences of images obtained by spectral analysis. Sequences were then analyzed by Factor Analysis of Medical Image Sequences (FAMIS) algorithm available via Pixies.[22,23] Therefore, emissions of MACS Texas Red and SYTOX Green in untreated HL1-NB cells screened by CLSM and available excitation sources can be differentiated. As a consequence, image analysis performed on spectral sequences of images leads to specific co-localized images of MACS Texas Red and SYTOX Green. Indeed, sequences of images can be investigated by FAMIS and provide factor images corresponding to each fluorescent compound. This method uses physical properties of fluorochromes, and permits the isolation of fluorochromes by means of their spectral pattern, as well as their velocity.

Image analysis

Following general factor analysis techniques, FAMIS was developed to process biomedical image sequences.[22,23] The FAMIS process has to cope with mixtures of components characterized by their physical behavior as well as linearity and component positivity basic hypothesis.

Sequences of images were further processed by FAMIS, available at Apteryx under the name of Pixies (www.apteryx.fr). FAMIS decomposes image sequences into a smaller number of images called factor images, and curves, called factor curves.[35,36] Factor curves estimate individual spectral or temporal behavior in the sequence of images. Factor images correspond to spatial distribution components. The basic idea of FAMIS is to process the curves that represent the evolution of fluorescence intensity of each pixel in the image spectral or temporal sequence (Figure 1). FAMIS assumes that each pixel is a mixture of different patterns and aims to unmix them. Factors are estimated in a two-step procedure from the image sequence.

Pixels of the images are combined into 4×4 clusters. Correspondence analysis[37,38] is first performed on the intensity evolution of each cluster. Then oblique analysis is performed on the results of correspondence analysis,[22] requiring positive factor curves and images. Factor images are recomputed in the original sampling by oblique projection, on the factor curves and the estimation is performed using the least-squares method. Here, the factor curves correspond to the emission spectra and the capture or staining kinetics of the fluorochromes. Factor

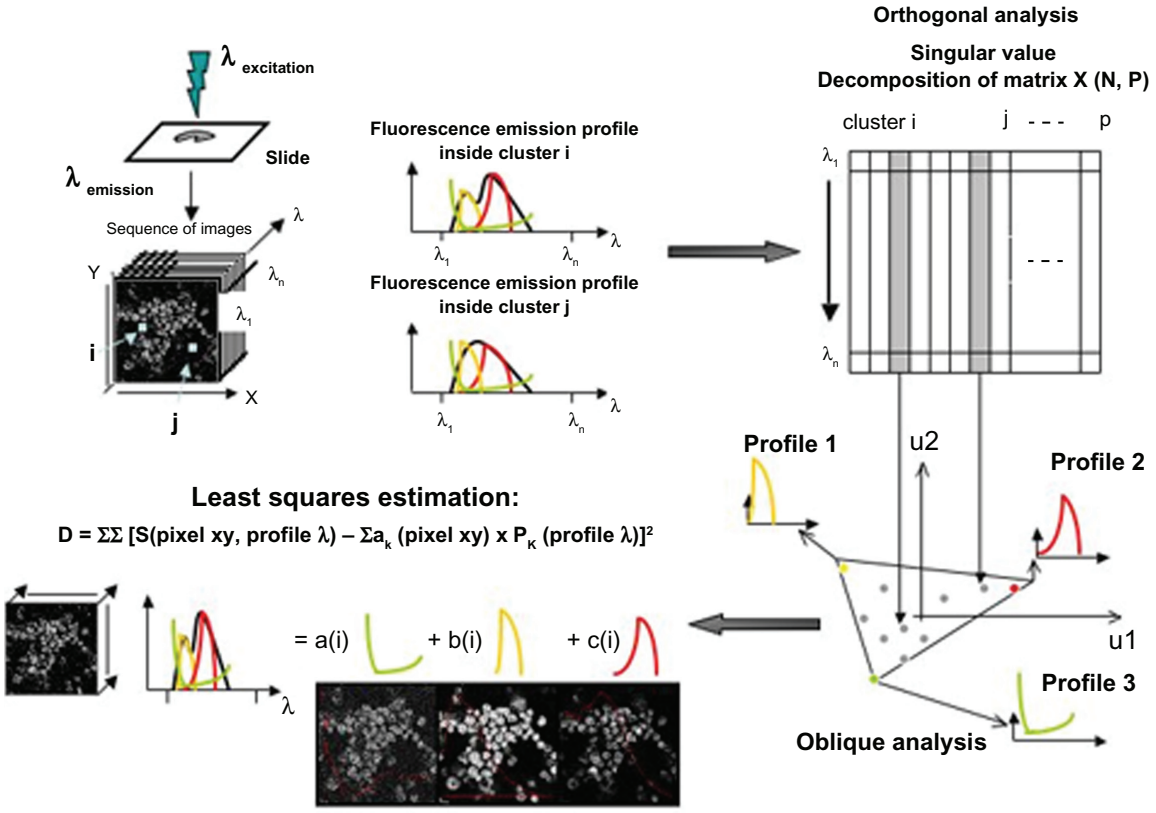

Figure 1 Basic presentation of FAMIS. Factors are estimated in a two-step procedure from the image sequence: 1) correspondence analysis and 2) oblique analysis are performed to obtain positive factor curves and images. Factor images are recomputed back to the original sampling by oblique projection on the factor curves.

images provide images of stained fluorescent structures. Superimposition in true color of these factor images provides a supplementary tool for interpretation.

Statistical analysis

Statistical analyses were performed on at least three independent experiments with SigmaStat 2.03 software (Systat Software Inc) with the Student t test. Data were considered statistically different at a *P* value of 0.05 or less.

Results

Confocal laser scanning microscopic analysis of iron nanoparticles in untreated or 7KC-treated HL1-NB cells counterstained with SYTOX Green

Action of MACS Texas Red iron nanoparticles on cells

In the case of spectral observations of MACS Texas Red treated cells (1: 6–10 h; 2: 20–24 h) in which emissions are collected through band-pass filters then processed before interpretation, the excitation at 488 nm and 514–532 nm was performed and emission was collected in the regular mode (515–550 nm, 590–621 nm) (Figure 2-A1; Figure 2-A2), and the spectral mode in 10 nm filters from blue to red (555 ≥ 705 nm). The resulting spectral sequences were investigated by means of FAMIS. A green emission corresponding to SYTOX Green is visualized in the first factor image and a red emission (610 nm) is visualized in the second factor image (Figure 2-B). Superimposition in true color of these factor images (Figure 2-C) provides a supplementary tool for interpretation.

Injection of MACS Texas Red iron nanoparticles on cells

In the case of temporal and spectral observations of MACS Texas Red nanoparticles injected in a culture of untreated cells in which emissions are collected through band-pass filters then processed before interpretation, the excitation at 488 nm and 514–532 nm was performed and emission was collected in the regular mode (515–550 nm, 590–621 nm) after injection (Figure 3-A). The emission was then collected in the spectral mode in 10 nm filters from blue to red (525 ≥ 715 nm) and subsequently in the temporal mode in a long pass filter (>525 nm). The resulting spectral and temporal sequences were investigated by means of FAMIS.

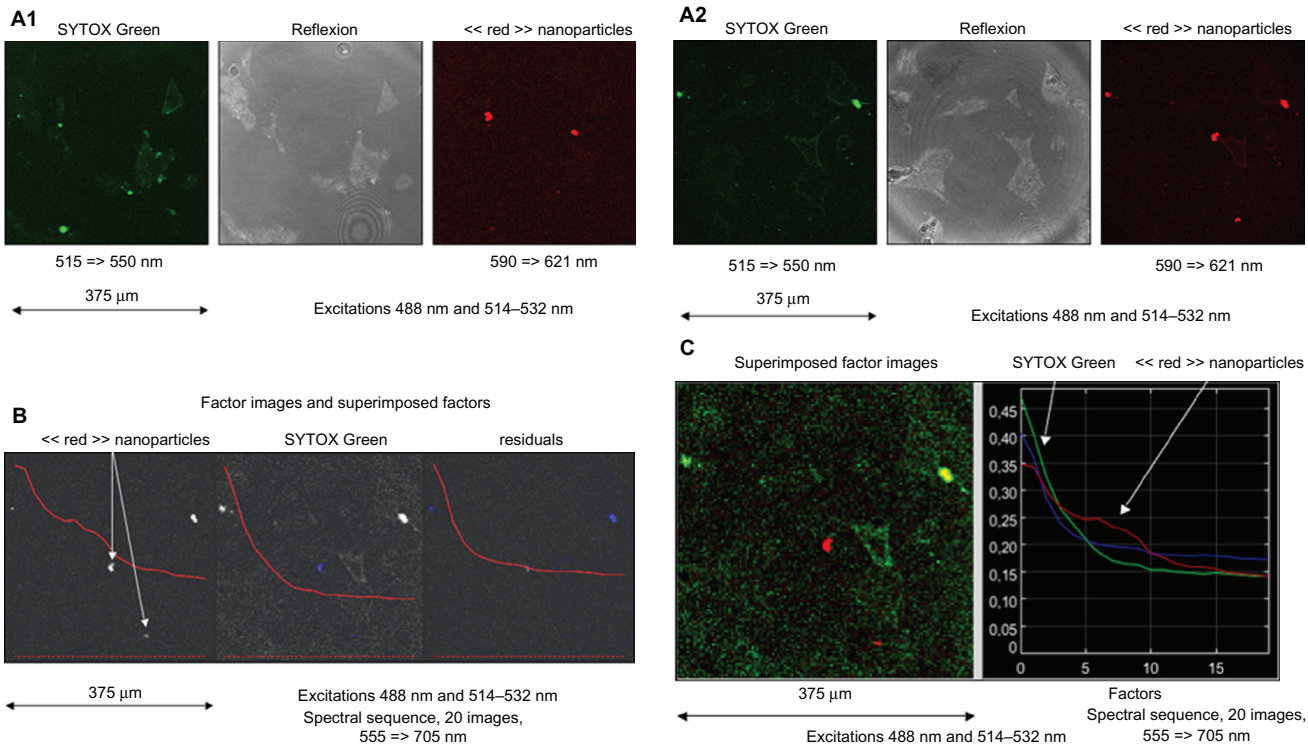

Figure 2 Case of spectral observations of iron nanoparticles conjugated with Texas Red incubated in untreated murine cardiac HL1-NB cells and counterstained with SYTOX Green (1: 6-10 h, 2: 20-24 h) in which emissions are collected through band-pass filters. **A1–A2**) Regular mode through band-pass filters. **B**) Spectral mode through 10 nm band-pass filters to obtain sequences of images and process by means of FAMIS. A green emission (535 nm) corresponding to SYTOX Green is visualized in the first factor image and a red emission (610 nm) is visualized in the second factor image. **C**) Superimposition in true color of these factor images.

Temporal sequence: a stable emission corresponding to SYTOX Green is visualized in the second and third factor images, and an emission uptake corresponding to Texas Red is visualized in the first factor image (Figure 3-B). Superimposition in true color of these factor images (Figure 3-C) provides a supplementary tool for interpretation.

Spectral sequence: a green emission (535 nm) corresponding to SYTOX Green is visualized in the first factor image and red emission (610 nm) is visualized in the second factor image (Figure 3-D). Superimposition in true color of these factor images (Figure 3-E) provides a supplementary tool for interpretation.

Action of 7KC with MACS Texas Red iron nanoparticles on cells

Spectral observations of 7KC treated cells (6–10 h; 20–24 h) were performed in which emissions were collected through band-pass filters and processed before interpretation, to visualize the possible toxicity of products by means of SYTOX Green. The excitation at 488 nm and 514–532 nm was performed and emission was collected in the regular mode (515–550 nm, 590–621 nm). Evidence of toxicity of 7KC at 20–24 h is thus obtained together with the nontoxicity of 7KC at 6–10 h (Figure 4). When 7KC is combined with MACS Texas Red iron nanoparticles to process cells, no higher toxicity could be visualized at 6–10 h. As for a comparison, evidence of higher toxicity on cells of decane (6 h) and europium chloride (1 h) at similar concentrations was demonstrated (data not shown), by using the same protocol. In these cases most of the cells did accumulate SYTOX Green.

Quantification of the cytotoxic, pro-inflammatory and pro-oxidative effects of iron nanoparticles associated or not with 7-ketocholesterol on HL1-NB cells

The ability of iron nanoparticles to induce cell death, and to trigger pro-inflammatory, and pro-oxidative effects on HL1-NB cells was evaluated comparatively to untreated cells (control), 7KC-, and (7KC + iron nanoparticles)-treated cells by using flow cytometric, biochemical and microscopic methods at 30 h of culture (Table 1). Compared to untreated cells, slight cytotoxic effects of iron nanoparticles were found in the presence of iron nanoparticles. These cytotoxic effects revealed by a significant increase of LDH release in the culture medium were not associated with an enhanced percentage of SYTOX Green positive cells (corresponding to dead cells). Moreover, no effects of iron nanoparticles were found on the levels of IL-8 and MCP-1. Indeed, similar levels of IL-8 and MCP-1 were found (Table 1) in the culture medium of untreated cells and of cells cultured in the presence of iron nanoparticles. It should be noted that in agreement with data obtained on promonocytic U937 cells,[31] significant cytotoxic and pro-oxidative effects were found on 7KC-treated HL1-NB cells whereas no pro-inflammatory activities were observed (Table 1). Interestingly, the ability of 7KC to induce cell death, overproduction of ROS, and IL-8 secretion was enhanced in the presence of iron nanoparticles (Table 1).

Discussion

The present study performed on living murine cardiac HL1-NB cells was carried out to identify the biological activities of fluorescent iron nanoparticles, and to evaluate whether they are able to induce cell death and stimulate the production of ROS and/or the secretion of cytokines (IL-8, MCP-1) capable of favoring the recruitment of monocytes, granulocytes, and T-cells, and therefore to promote inflammatory processes.[31,39] As it has been reported that exposure to ambient air nanoparticles can increase peripheral thrombosis, and atherosclerotic lesion formation,[40] additional investigations are important to evaluate the contribution of nanoparticles to specific aspects of cardiovascular diseases, and to determine whether nanoparticles can influence major cardiovascular risk factors, such as diabetes, hypertension, cholesterol as well as some of its main oxidized derivatives such as 7KC which plays a major part in cardiovascular diseases.[41,42] Therefore, the present study was undertaken on living cardiomyocytes (HL1-NB cells) to better understand the response of cardiac cells when they are exposed to iron nanoparticles in the absence or in the presence of 7KC.

To this end, flow cytometric and confocal microscopic methods of investigation were used. Cell viability, analyzed by means of staining with SYTOX Green, was also evaluated by measuring the release of lactate deshydrogenase (LDH) in the culture medium.[30,43] Pro-inflammatory effects were evaluated by measuring IL-8 and MCP-1 secretion in the culture medium,[43] and overproduction of ROS was quantified by flow cytometry after staining with HE.[33,34] Confocal observations were made more effective and specific by using the sequences of images that can be obtained by spectral or temporal modes, and were then processed by image analysis. Indeed, factor analysis (FAMIS) makes it possible to differentiate spectral or temporal emissions of fluorochromes in a multistaining system and to provide the images corresponding to each fluorochrome.[44] The use of the FAMIS image processing

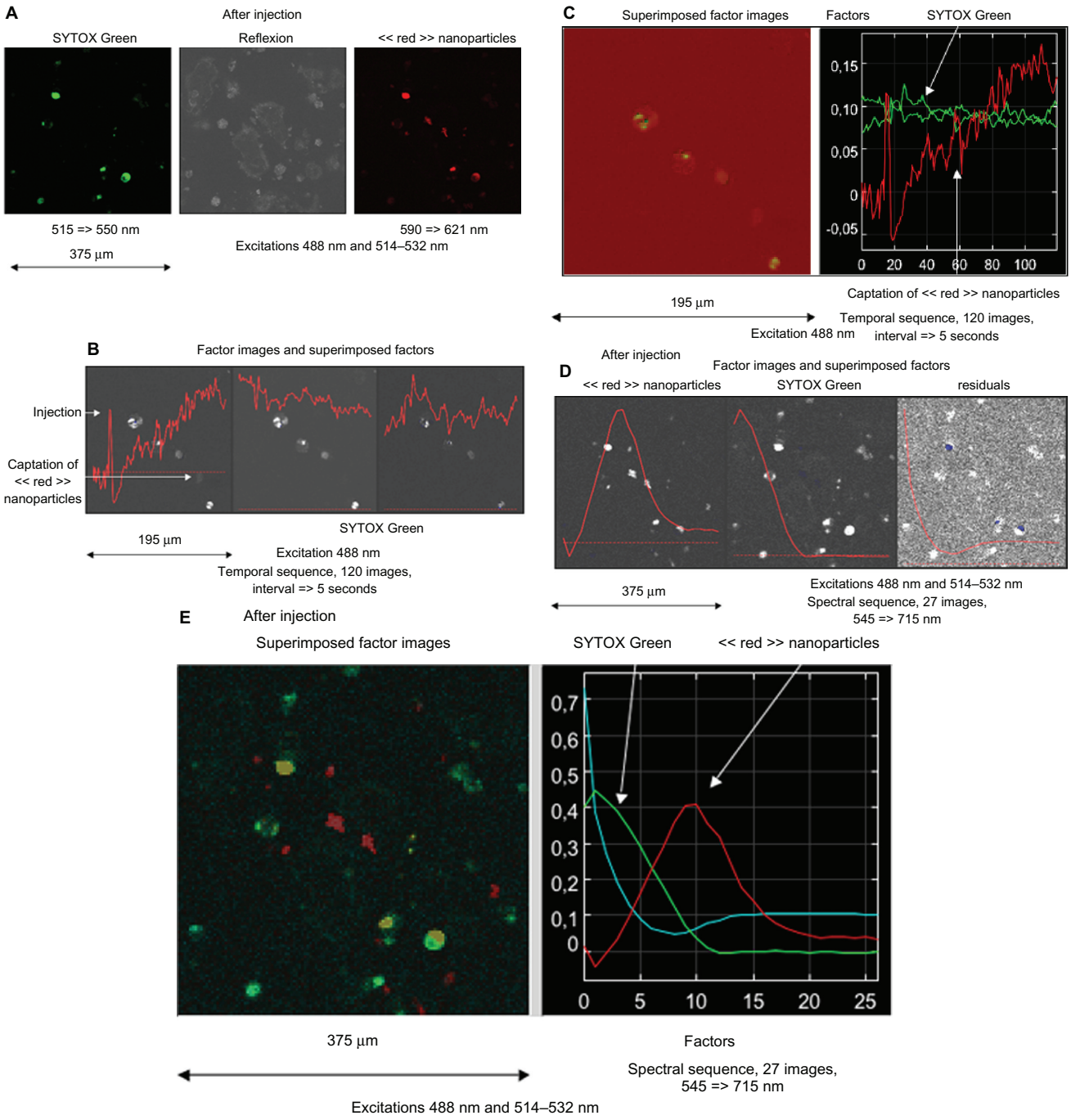

Figure 3 Case of temporal and spectral observations of iron nanoparticles conjugated with Texas Red injected in a culture of untreated murine cardiac HL1-NB cells counterstained with SYTOX Green in which emissions are collected through band-pass filters. **A**) Regular mode through band-pass filters after injection. **B**) The emission is then collected in the temporal mode in a long-pass-filter and processed by means of FAMIS.A stable emission corresponding to SYTOX Green and an emission uptake corresponding to red nanoparticles are visualized to localize nanoparticles in cell compartments. **C**) Superimposition in true color of the factor image. In some cells, the presence of a high signal emphasizes the fact that nanoparticles accumulate inside cytoplasm. **D**) Spectral mode through 10 nm band-pass filters. Investigation by means of FAMIS.A green emission (535 nm) corresponding to SYTOX Green in the first factor image and a red emission (610 nm) corresponding to red nanoparticles are visualized in the second factor image. Nanoparticles are either captured or not by the cells. **E**) Superimposition in true color of these factor images is performed to localize nanoparticles in cell compartments.

technique also allows the differentiation of mixed fluorescent emissions from dyes and nanoparticles,[45] and factor images make it possible to obtain an overview of the uptake and effect of nanoparticles at the single cell level.[46]

Since nanoparticles can interact with various molecules, receptors, and/or macromolecular complexes, iron nanoparticles can contribute to activate, repress, or modulate some metabolic pathways. As the early biological activities of

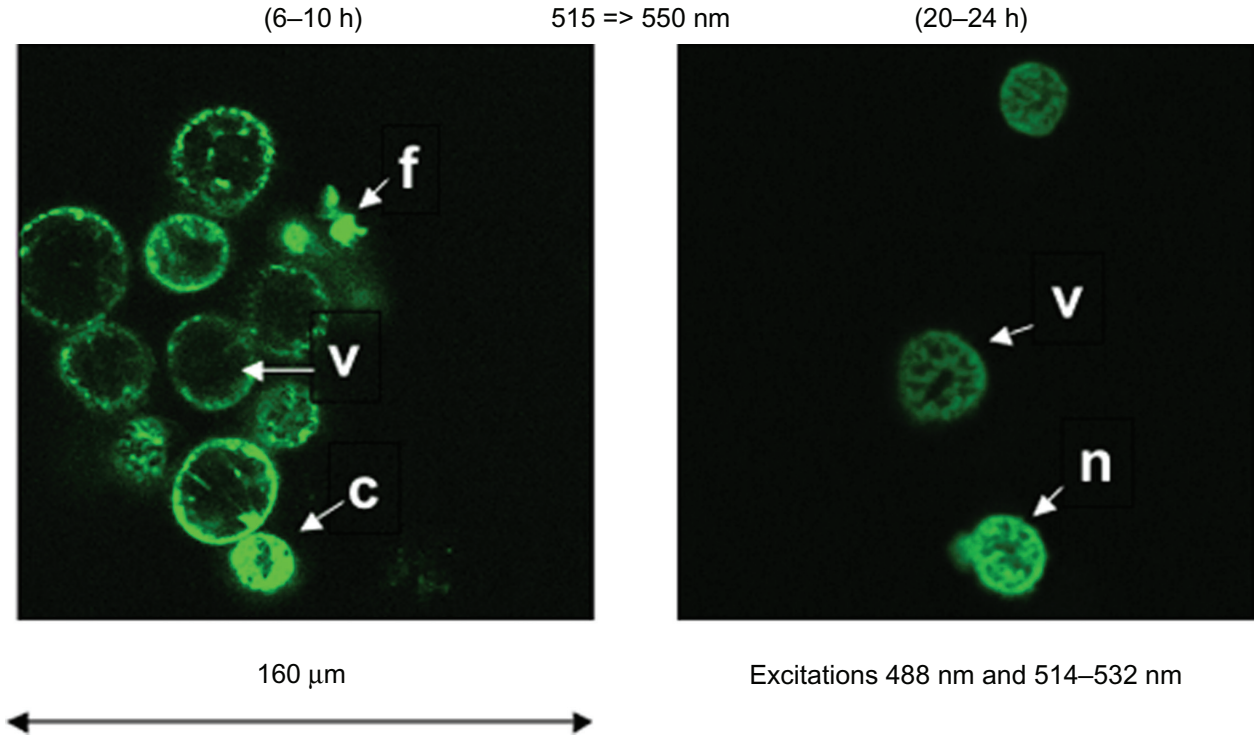

Figure 4 Case of spectral observation of the action of 7-ketocholesterol on murine cardiomyocytes HL1-NB cells counterstained with SYTOX Green. Spectral observations of 7-ketocholesterol-treated cells (6-10 h; 20-24 h) show the possible toxicity of products by means of SYTOX Green. At 6–10 h, most visible cells are viable (**v**), but typical figures of apoptosis are also observed (cells with condensed (**c**) or fragmented (**f**) nuclei), probably corresponding to spontaneous apoptosis. At 20–24 h, the structure of the nuclei suggests necrosis (**n**), which can either correspond to primary or secondary necrosis.[7,17]

7KC on the cytoplasmic membrane involves the PDK1/Akt signalling pathway,[47] which subsequently activates various signalling pathways (especially those triggering cell death),[17] it is important to determine whether iron nanoparticles interacting with the cytoplasmic membrane are able to modulate some biological activities of 7KC strongly suspected to play important roles in cardiovascular diseases. Noteworthy, our data show that these iron nanoparticles have slight cytotoxic activities, and that they do not trigger the release of major chemokines, such as IL-8 and MC-P1, known to favor the recruitment of inflammatory cells into the vascular wall contributing therefore to the development of vascular lesions.[43,30] Moreover, iron nanoparticles do not stimulate the production of ROS. However, interaction of iron nanoparticles with murine cardiac HL1-NB cells increases 7KC induced cell death, inflammation, and oxidation. Indeed, an increased proportion of SYTOX Green positive cells and higher levels of LDH release were observed, and IL-8 secretion, and ROS production were significantly enhanced. Thus, whereas additional *in vivo*

Table 1 Evaluation of the cytotoxic, pro-inflammatory, and pro-oxidative effects of iron nanobeads associated or not with 7-ketocholesterol on murine cardiomyocytes HL1-NB

Assays	Control	Iron nanoparticles	7KC	7KC + iron nanoparticles
% SYTOX Green positive cells	11 ± 2	9 ± 1	51 ± 6*	61 ± 6**
LDH (U/L)	328 ± 1	346 ± 9*	348 ± 8*	353 ± 7
IL-8 (pg/mL)	16.0 ± 5.4	25.0 ± 10.0	16.0 ± 5.0	32.0 ± 10.0**
MCP-1 (pg/mL)	16.0 ± 5.0	15.0 ± 14.0	17.0 ± 5.0	16.0 ± 10.0
MFI of HE positive cells	15 ± 1	12 ± 1	20 ± 1*	25 ± 1**

Notes: Murine cardiac HL-1NB cells were cultured in the absence (control) or in the presence of iron nanoparticles associated or not with 7-ketocholesterol (7KC) for 30 h. At the end of the incubation time, the cytotoxic, pro-inflammatory and oxidative effects were evaluated by various methods: determination of the percentages of SYTOX Green positive cells (dead cells) by flow cytometry; quantification of LDH release in the culture medium; quantification by ELISA of the secretion of IL-8 and MCP-1 in the culture medium; measurement of the mean fluorescence intensity (MFI) of hydroethidine (HE) positive cells by flow cytometry. Data are mean ± standard deviation of three independent experiments. Significance of the differences between control and iron nanoparticles or 7KC-treated cells (*$P < 0.05$); 7KC and (7KC + iron nanoparticles)-treated cells (**$P < 0.05$).

experiments will be required to establish that lipid disorders can influence the biological activities of nanoparticles, our data highlight that iron nanoparticles are able to increase the side effects of a major cholesterol oxide derivative: 7KC. As iron nanoparticles are widely used for *in vivo* imaging,[48,49] our data suggest that they could be used with caution in atherosclerotic patients, who often have high risk of cardiovascular diseases.

Considering the results obtained from the evaluation of the ability of nanoparticles to promote cell death, pro-inflammatory and/or pro-oxidative processes, cellular deposits were used to perform CLSM analysis in order to link cell death (evaluated by means of SYTOX Green staining) with the accumulation of iron nanoparticles of untreated HL1-NB cells. In our conditions, we specifically screened the injection of iron nanoparticles in the culture medium of untreated and 7KC-treated cells. It resulted in temporal sequences of images, which were investigated by means of FAMIS. A green emission (535 nm) corresponding to SYTOX Green was observed inside cells together with the red emission (610 nm) of nanoparticles. This analysis provides information on the localization of the nanoparticles, and shows that they accumulate in cells. This combined spectral and temporal analysis of SYTOX Green and fluorescent nanoparticles makes the characterization of the interaction of nanoparticles on cells more specific. In processed confocal sequences of images, the repartition dynamics of nanoparticles is also determined, and the emission spectra of SYTOX Green and nanoparticles are differentiated. Computed dynamic and emission curves (factors) and corresponding factor images also show that the nanoparticles are localized at the periphery and inside the cardiac HL1-NB cells. As the biological activity of 7KC is associated with its accumulation in the cytoplasmic membrane, especially in lipid rafts,[50] the interaction of iron nanoparticles with the cytoplasmic membrane can explain their ability to modulate the effects of 7KC. The results obtained in the present investigation also indicate that the different methods tested in this study can be applied to characterize other iron nanoparticles such as ultra small iron oxide particles (USPIOs) frequently used to perform magnetic resonance imaging (MRI) of humans and animals.[51] Though we can not exclude that the labeling procedure can influence the cellular interactions and the biological activities of the iron nanoparticles that we tested, our approach can constitute a useful tool to early evaluate the possible side effects carried by nanoparticles such as USPIOs (Endorem, Sinerem [Guerbet, France]), which are used to improve MRI clinical investigations.

In conclusion, the combined use of FCM associated with appropriate biochemical and immunological methods, together with CLSM and subsequent spectral methods of analysis such as FAMIS, provide an efficient tool to analyze the interaction and the capture of nanoparticles by living cells, and to determine their abilities to promote cell death, and pro-inflammatory activities. This approach can be generalized and be used as an *in vitro* model to characterize side effects of various types of nanoparticles,[52] and has some applications in human toxicology. In addition, our data underline that the simultaneous use of CLSM with FAMIS is an efficient tool to differentiate colors in a designed multistaining system involving SYTOX Green and nanoparticles. Therefore, the proposed approach opens the way to numerous basic investigations with nanoparticles, allows the visualization of the cellular and the tissue distribution of various molecules associated with nanoparticles, and provides a valuable approach to evaluate the cytotoxic activities of various fluorescent nanoparticles on living cells and on small animal models.

Acknowledgments

This work was supported by the Institut National de la Santé et de la Recherche Médicale (INSERM), the Fondation de France, the University Hospital (CHU Dijon, France), and the Université de Bourgogne (Dijon, France).

Disclosures

The authors declare no conflicts of interest.

References

1. Bruchez M, Moronne M, Gin, P, Weiss S, Alivisatos AP. Semiconductor nanocrystals as fluorescent biological labels. *Science*. 1998; 281:2013–2016.
2. Taton T, Mirkin C, Letsinger R. Scanometric DNA array detection with nanoparticle probes. *Science*. 2000;289:1757–1760.
3. Cui Y, Wei Q, Park H, Lieber C. Nanowire nanosensors for highly sensitive and selective detection of biological and chemical species. *Science*. 2001;293:1289–1292.
4. Colvin V. The potential environmental impacts of engineered nanomaterials. *Nature Biotechnology*. 2003;21:1166–1170.
5. Murthy SK. Nanoparticles in modern medicine: state of the art and future challenges. *Int J Nanomedicine.* 2007;2:129–141.
6. Weber WA, Czernin J, Phelps ME, Herschman HR. Technology Insight: novel imaging of molecular targets is an emerging area crucial to the development of targeted drugs. *Nat Clin Pract Oncol*. 2008;5:44–54.
7. Vejux A, Lizard G. Cytotoxic effects of oxysterols associated with human diseases: Induction of cell death (apoptosis and/or oncosis), oxidative and inflammatory activities, and phospholipidosis. *Mol Aspects Med*. 2009;30:153–170.
8. Stroh A, Zimmer C, Gutzeit C, et al. Iron oxide particles for molecular magnetic resonance imaging cause transient oxidative stress in rat macrophages. *Free Radic Biol Med*. 2004;36:976–984.

9. Peters K, Unger RE, Gatti AM, Sabbioni E, Tsaryk R, Kirkpatrick CJ. Metallic nanoparticles exhibit paradoxical effects on oxidative stress and pro-inflammatory response in endothelial cells in vitro. *Int J Immunopathol Pharmacol.* 2007;20:685–695.
10. Hussain SM, Hess KL, Gearhart JM, Geiss KT, Schlager JJ. In vitro toxicity of nanoparticles in BRL 3A rat liver cells. *Toxicol In Vitro*. 2005;19:975–983.
11. Tsuji JS, Maynard AD, Howard PC, et al. Research strategies for safety evaluation of nanomaterials, part IV: risk assessment of nanoparticles. *Toxicol Sci*. 2006;89:42–50.
12. Oberdörster E. Manufactured nanomaterials (Fullerenes, C60) induce oxidative stress in the brain of juvenile largemouth bass. *Environmental Health Perspectives*. 2004;112:1058–1062.
13. Kolosnjaj J, Szwarc H, Moussa F. Toxicity studies of fullerenes and derivatives. *Adv Exp Med Biol.* 2007;620:168–180.
14. Oberdörster G, Oberdörster E, Oberdörster J. Nanotoxicology: an emerging discipline evolving from studies of ultrafine particles. *Environ Health Perspect*. 2005;113:823–839.
15. Kumar V, Farell G, Yu S, et al. Cell biology of pathologic renal calcification: contribution of crystal transcytosis, cell mediated calcification, and nanoparticles. *J Investig Med*. 2006; 54:412–424.
16. Tetley TD. Health effects of nanomaterials. *Biochem Soc Trans*. 2007;35(Pt 3):527–531.
17. Vejux A, Malvitte L, Lizard G. Side effects of oxysterols: cytotoxicity, oxidation, inflammation, and phospholipidosis. *Braz J Med Biol Res*. 2008;41:545–556.
18. Lukyanenko V, Lukyanenko Y. Oxysterols in heart failure. *Future Cardiol*. 2009;5:343–354.
19. Corot C, Robert P, Idée JM, Port M. Recent advances in iron oxide nanocrystal technology for medical imaging. *Adv Drug Deliv Rev*. 2006; 58:1471–1504.
20. Claycomb WC, Lanson NA, Stallworth BS, et al. HL-1 cells: a cardiac muscle cell line that contracts and retains phenotypic characteristics of the adult cardiomyocytes. *Proc Natl Acad Sci U S A.* 1998; 95:2979–2984.
21. Pelloux S, Robillard J, Ferrera R, et al. Non-beating HL-1 cells for confocal microscopy: application to mitochondrial functions during cardiac preconditioning. *Prog Biophys Mol Biol*. 2006; 90:270–298.
22. Di Paola R, Bazin JP, Aubry F, et al. Handling of dynamic sequences in nuclear medecine. *IEEE Trans Nucl Sci*. 1982; 29:1310–1321.
23. Frouin F, Cinotti L, Benali H, et al. Extraction of functional volumes from medical dynamic volumetric datasets. *Comp Med Imaging Graph*. 1993;17:397–404.
24. Vejux A, Lizard G, Tourneur Y, Riedinger JM, Frouin F, Kahn E. Effects of caspase inhibitors (z-VAD-fmk, z-VDVAD-fmk) on Nile Red fluorescence pattern in 7-ketocholesterol-treated cells: investigation by flow cytometry and spectral imaging microscopy. *Cytometry A*. 2007;71:550–562.
25. Kahn E. Confocal microscopy: characterization of fluorescent tracers by image processing of optical sections. *Pathol Biol*. 2001; 49:194–198.
26. Kawata S, Sasaki K, Minami S. Component analysis of spatial and spectral patterns in multispectral images I Basis. *JOSA A*. 1987; 4:2101–2106.
27. Lansing Taylor D, Waggoner AS, Murphy RF, Lanni F, Birge RR. *Applications of Fluorescence in the Biomedical Sciences*. New York: Alan R Liss Inc; 1986:129–140.
28. de la Monte SM, Neely TR, Cannon J, Wands JR. Ethanol impairs insulin-stimulated mitochondrial function in cerebellar granule neurons. *Cell Mol Life Sci*. 2001;58:1950–1960.
29. Cirelli N, Lebrun P, Gueuning C, et al. Secretory characteristics and viability of human term placental tissue after overnight cold preservation. *Hum Reprod*. 2000;15:756–761.
30. Prunet C, Montange T, Véjux A, et al. Multiplexed flow cytometric analyses of pro- and anti-inflammatory cytokines in the culture media of oxysterol-treated human monocytic cells and in the sera of atherosclerotic patients. *Cytometry A*. 2006;69:359–373.
31. Lemaire-Ewing S, Prunet C, Montange T, et al. Comparison of the cytotoxic, pro-oxidant and pro-inflammatory characteristics of different oxysterols. *Cell Biol Toxicol*. 2005;91:97–114.
32. Moldrich RX, Beart PM, Pascoe CJ, Cheung NS. Low-affinity kainate receptor agonists induce insult-dependent apoptosis and necrosis in cultured murine cortical neurons. *J Neurosci Res*. 2000;59:788–796.
33. Rothe G, Valet G. Flow cytometric analysis of respiratory burst activity in phagocytes with hydroethidine and 2',7'-dichlorofluorescin. *J Leukoc Biol*. 1990;47:440–448.
34. Rothe G, Valet G. Flow cytometric assays of oxidative burst activity in phagocytes. *Methods Enzymol*. 1994;233:539–548.
35. Kahn E, Frouin F, Souchier C, et al. Confocal multilaser focusing and single-laser characterization of UV excitable stains of cellular preparations. *Cytometry*. 2000;40:42–49.
36. Kahn E, Lizard G, Pélégrini M, et al. Four-dimensional factor analysis of confocal images sequences (4D-FAMIS) to detect and characterize low numbers of human papillomavirus DNA by FISH in HeLa and SiHa cells. *J Microscopy*. 1999;193:227–243.
37. Harman HH. *Modern Factor Analysis*. Chicago: University of Chicago Press; 1960.
38. Benzecri JP. *L'analyse des Données, Tome 2: L'analyse des Correspondances*. Paris: Dunod; 1973.
39. Lizard G, Gueldry S, Sordet O, et al. Gluthatione is implied in the control of 7-ketocholesterol-induced apoptosis, which is associated with radical oxygen species production. *FASEB J*. 1998; 12:1651–1663.
40. Bhatnagar A. Environmental cardiology. Studying mechanistic links between pollution and heart disease. *Circ Res*. 2006; 99:692–705.
41. Brown AJ, Jessup W. Oxysterols and atherosclerosis. *Atherosclerosis*. 1999;142:1–28.
42. Van Reyk DM, Brown AJ, Hult'en LM, Dean RT, Jessup W. Oxysterols in biological systems: sources, metabolism and pathophysiological relevance. *Redox Rep*. 2006;11:255–262.
43. Lemaire S, Lizard G, Monier S, et al. Different patterns of IL-1beta secretion, adhesion molecule expression and apoptosis induction in human endothelial cells treated with 7alpha-, 7beta-hydroxycholesterol, or 7-ketocholesterol. *FEBS Lett*. 1998;440:434–439.
44. Kahn E, Hotmar J, Frouin F, et al. Spectral and dynamic confocal fluorescence characterization of cytogenetic preparations by factor analysis. *Anal Cell Pathol*. 1996;12:45–56.
45. Kahn E, Receveur A, Coullin P, et al. Multiple excitation confocal analysis of targets in nuclei of cytogenetic preparations. *Anal Quant Cytol Histol*. 2004;26:1–7.
46. Kahn E, Vejux A, Menetrier F, et al. Analysis of CD36 expression on human monocytic cells and atherosclerotic tissue sections with quantum dots. Investigation by flow cytometry and spectral imaging microscopy. *Anal Quant Cytol Histol*. 2006;28:14–26.
47. Vejux A, Guyot S, Montange T, Riedinger JM, Kahn E, Lizard G. Phospholipidosis and down-regulation of the PI3-K/PDK-1/Akt signalling pathway are vitamin E inhibitable events associated with 7-ketocholesterol-induced apoptosis. *J Nutr Biochem*. 2009; 20:45–61.
48. Michalet X, Pinaud FF, Bentolila LA, et al. Quantum dots for live cells, in vivo imaging, and diagnostics. *Science*. 2005;307:538–544.
49. Gao X, Dave SR. Quantum dots for cancer molecular imaging. *Adv Exp Med Biol*. 2007;620:57–73.
50. Royer MC, Lemaire-Ewing S, Desrumaux C, et al. 7-ketocholesterol incorporation into sphingolipid/cholesterol-enriched (lipid raft) domains is impaired by vitamin E: a specific role for alpha-tocopherol with consequences on cell death. *J Biol Chem*. 2009; 284:15826–15834.

51. Di Marco M, Sadun C, Port M, Guilbert I, Couvreur P, Dubernet C. Physicochemical characterization of ultrasmall superparamagnetic iron oxide particles (USPIO) for biomedical application as MRI contrast agents. *Int J Nanomedicine*. 2007;2:609–622.

52. Auffan M, Rose J, Bottero JY, Lowry GV, Jolivet JP, Wiesner MR. Towards a definition of inorganic nanoparticles from an environmental, health and safety perspective. *Nat Nanotechnol*. 2009;4:634–641.